Journal of Electronic Materials

The role of defects on the resistive switching behavior of Ta2O5-TiO2 based metal-insulator-metal (MIM) devices for memory applications

--Manuscript Draft--

Manuscript Number:	JEMS-D-17-01470R1
Full Title:	The role of defects on the resistive switching behavior of Ta2O5-TiO2 based metal-insulator-metal (MIM) devices for memory applications
Article Type:	S.I. : 2017-DRIP
Keywords:	Resistive switching; tantalum oxide: titanium oxide; Defects; metal-insulator-metal; high-k dielectric stacks.
Corresponding Author:	Salvador Dueñas Universidad de Valladolid Valladolid, SPAIN
Corresponding Author Secondary Information:	
Corresponding Author's Institution:	Universidad de Valladolid
Corresponding Author's Secondary Institution:	
First Author:	Salvador Dueñas
First Author Secondary Information:	
Order of Authors:	Salvador Dueñas
	Helena Castan
	Héctor García
	Óscar G. Ossorio
	Luis A. Domínguez
	Helina Seemen
	Aile Tamm
	Kaupo Kukli
	Jaan Aarik
Order of Authors Secondary Information:	
Funding Information:	Ministerio de Economía y Competitividad (TEC2014-52152-C3-3-R) — Dr. Helena Castan
	Estonian Research Agency (PUT170) — Dr. Aile Tamm
	Estonian Research Agency (IUT2-24) — Dr. Kaupo Kukli
	European Regional Development Fund (TK134) — Dr. Aile Tamm
	European Regional Development Fund (TK141) — Dr. Kaupo Kukli
Abstract:	In this work we describe the role of defects on the resistive switching behavior of metal-insulator-metal devices based on alternating Ta2O5 and TiO2 stacks. Ruthenium oxide, RuOx, and platinum, Pt, were used as bottom and top electrodes, respectively. 5 nm-thick insulator stacks were fabricated by atomic layer deposition of alternating Ta2O5 and TiO2 thin films. Bipolar resistive switching behavior was obtained on Ta2O5-TiO2-Ta2O5 and TiO2-Ta2O5-TiO2 stacks. The best memristive response was obtained in the case of two TiO2 films embedding a monolayer of Ta2O5. Very repetitive dc current-voltage bipolar switching cycles were obtained. Small signal

Powered by Editorial Manager® and ProduXion Manager® from Aries Systems Corporation

	admittance parameters also showed hysteretic behavior during a whole bipolar switching cycle. In the case of samples with three layers of similar thickness, when the transition from the ON to the OFF state (Reset) occurs, the conductance abruptly increases and the susceptance experiences fast decreasing for more negative voltages values. Such behavior was not observed when only one Ta2O5 monolayer was examined. These differences are explained in terms of charge transport mechanism occurring in the open conductive filaments.

Powered by Editorial Manager® and ProduXion Manager® from Aries Systems Corporation

LIST OF CHANGES Ms. Ref. No.: Manuscript #JEMS-D-17-01470

Title: **The role of defects on the resistive switching behavior of Ta_2O_5-TiO_2 based metal-insulator-metal (MIM) devices for memory applications**

First, we want to thank the two reviewers for their clever comments and suggestions.

In the following we enumerate the changes we made in the manuscript to accomplish the reviewers as well as the Editorial Office comments. Due to the paper limits for this special number of the journal, we have also tried to do not extend too much the manuscript extension.

1. COMMENTS TO THE AUTHOR:

Reviewer #1: This short paper is well written considering the space restrictions. The bilayer structure approach is described in a succinct manner. The only thing that I want to see in next revision is to have author add a cross sectional SEM /TEM image of the structure. That will give this paper more visibility to scientific community.
A new Figure (Figure 3 in the revised version) showing SEM micrographs of all samples have been added. A comment about this Figure has been added at the end of SAMPLE DESCRIPTION section. Figures 3 to 6 have been accordingly renumbered.

Reviewer #2: 1. It will be better if all the samples should be summarized in a table with the details and names.
A sample summary has been included in Table I.
2. Authors mentioned that the role of density of defects is crucial, so it is expected that they must inform about it too. which kind of defects they have studied? meanwhile on micro-structural level the insulator stack is already amorphous.
Some brief sentences has been included in Abstract (line 5) and in the Conclusions, in which we identify oxygen vacancies as responsible for the RS behavior.

3. Did authors try to give post deposition heat treatment to the sandwiched layer? may possible it show crystalline behavior, will there any effect on performance if it so?
See the sentence added at the end of SAMPLE DESCRIPTION section.

4. authors mentioned that the switching between low resistance to high resistance is occurs due to oxygen vacancies, it is mentioned that during the positive voltage oxygen vacancies created, are these disappeared by negative voltage sweep, so there is high resistance?

We have modified the last paragraph of Page 5 to clarify this question.

2. Editorial Office Comments:

**Define all acronyms on first use in the abstract and again in the body of the manuscript using this style:
molecular beam epitaxy (MBE). Do not capitalize words in the definitions unnecessarily unless they are proper names or at the beginning of a sentence. For example, dc in the abstract.
The entire manuscript has been carefully revised to correct acronyms.

**Figure 1: Please correct the spelling of the y axis. It should be “Intensity, arb. units” not “Intesity”

**Figure 5 requires correction. Put figure panel labels (a, b, etc.) on the figure itself. Do not place beside the figure.

Figure 1 and old Figure 5 (now Figure 6) have been corrected.

Marked Manuscript

The role of defects on the resistive switching behavior of Ta_2O_5-TiO_2 based metal-insulator-metal (MIM) devices for memory applications

S. DUEÑAS[1,4], H. CASTÁN[1], H. GARCÍA[1], O. G. OSSORIO[1], L. A. DOMÍNGUEZ[1],

H. SEEMEN[2], A. TAMM[2], K. KUKLI[2,3], and J. AARIK[2]

1.- Department of Electronics, University of Valladolid, Campus Miguel Delibes, 47011 Valladolid, Spain

2.- Institute of Physics, University of Tartu, W. Ostwald 1, 50411 Tartu, Estonia

3.- Department of Chemistry, University of Helsinki, P.O. Box 55, FI-00014 Helsinki, Finland

4.- e-mail: sduenas@ele.uva.es

ABSTRACT

In this work we describe the role of defects on the resistive switching behavior of metal-insulator-metal devices based on alternating Ta_2O_5 and TiO_2 stacks. Ruthenium oxide, RuO_x, and platinum, Pt, were used as bottom and top electrodes, respectively. 5 nm-thick insulator stacks were fabricated by atomic layer deposition of alternating Ta_2O_5 and TiO_2 thin films. Bipolar resistive switching behavior was obtained on Ta_2O_5-TiO_2-Ta_2O_5 and TiO_2-Ta_2O_5-TiO_2 stacks. These behavior is mainly due to the presence of oxygen vacancy defects. The best memristive response was obtained in the case of two TiO_2 films embedding a monolayer of Ta_2O_5. Very repetitive direct current (dc) -voltage bipolar switching cycles were obtained. Small signal admittance parameters also showed hysteretic behavior during a whole bipolar switching cycle. In the case of samples with three layers of similar thickness, when the transition from the ON to the OFF state (Reset) occurs, the conductance abruptly increases and the susceptance experiences fast decreasing for more negative voltages values. Such behavior was not observed when only one Ta_2O_5 monolayer was examined. These differences are explained in terms of charge transport mechanism occurring in the open conductive filaments.

KEY WORDS: Resistive switching, tantalum oxide, titanium oxide, defects, metal-insulator-metal, high-k dielectric stacks.

INTRODUCTION

Resistive random-access memories (RRAM) are nowadays very well reputed challengers to fabricate low power, high density and high endurance nonvolatile memories (NVM) [1-2]. An additional advantage of RRAMs is the possibility to become fabricated as three-dimensional cross bar arrays (CBA). They are based on the memristive properties of various insulators, including binary oxides, perovskites, nitrides and selenides [3-7]. RRAMs working principle is based on the reversible formation and rupture of single or multiple nanoconfined conductive filaments (CF) between the two electrodes of a metal-insulator-metal (MIM) or metal-insulator-semiconductor (MIS) structure. The conductive filaments are formed by the accumulation of defects (metallic atoms, or oxygen vacancies, for instance) throughout the insulator. Based on the nature of the defects and the principal operation mechanisms of resistive switching, different kind of RRAMs can be obtained: valence change memory (VCM), electrochemical metallization memory (ECM), or thermochemical memory (TCM). The VCM memories are based on redox reactions which yield the creation and migration of oxygen vacancies through networks of defects and change the conductivity. This mechanism usually produces bipolar switching devices. ECM and TCM memories are based on the combination of redox reactions and Joule heating in the filament and its neighboring regions. Metallic filaments are created during the electroforming and are interrupted by electric field assisted Joule heating during the Reset pulse. Subsequent Joule heating-assisted reduction of the interrupted filament rebuilds the filament so switching the device to the conductive state (Set). Both mechanisms can be achieved with the same bias polarity (unipolar switching behavior).

During the last decade a variety of high permittivity oxides, e.g. HfO_2, ZrO_2, TiO_2, Ta_2O_5, $SrTiO_3$, NiO, have been proposed as challengers for resistive switching [8]. To reach an accurate control of RRAM devices, an in-depth knowledge about the role and density of defects on the CF formation and dilution is mandatory. Moreover, the potential applications of high-k based RRAMs requires a careful design of the switching layer structure to obtain RRAM devices with excellent performance and reliability. Due to the expected high density of RRAMs, low power consumption and good uniformity must be warranted. To reduce power consumption, several methods have been proposed, such as using bilayer structure and device area scaling [9-13]. The bilayer structure is considered as the most promising approach, and the improved characteristics of these bilayer devices are displayed adequately [11,12]. Some high-k dielectrics exhibit good resistive switching behavior. Others are not so good in terms of switching, but are better in terms of leakage current and thermodynamic stability. The combination of materials having complementary properties is the key for the interest in bilayer structures [14].

In this work, resistive switching phenomena on Ta_2O_5 and TiO_2 multilayers based metal-insulator-metal (MIM) structures are reported. Ta_2O_5-TiO_2 films were grown to target thickness of 5 nm. The films were grown either as multilayer stacks of Ta_2O_5 and TiO_2 or TiO_2 films embedding a monolayer of Ta_2O_5. The stacks were grown to stabilize the conductive filaments in TiO_2 by inserting otherwise more insulating tantalum oxide, and examine the possible effect of layering different metal oxides on the resulting RRAM devices.

SAMPLE DESCRIPTION

MIM samples were obtained by depositing the films on 15 nm-RuO_2/10 nm-TiN/Si substrates. Oxide films were grown in an in-house built low-pressure flow-type atomic-layer-deposition (ALD) reactor [15, 16] in the form of stacks consisting of TiO_2-Ta_2O_5-TiO_2 or Ta_2O_5-TiO_2-Ta_2O_5 triple layers at the substrate temperature of 350 ºC. Metal chloride precursors, $TiCl_4$ and $TaCl_5$, were used to grow TiO_2 and Ta_2O_5, respectively. Ozone was used as oxygen precursor. TiO_2 layers were grown using cycle times 2-2-5-5 s, denoting sequence of $TiCl_4$ pulse length – purge time - ozone pulse length - purge time, respectively. For Ta_2O_5, the corresponding cycle times were 3-2-5-5 s. Four different multilayer structures of alternating Ta_2O_5 and TiO_2 were fabricated. First, a three-layer Ta_2O_5-TiO_2-Ta_2O_5 were fabricated with a sequence of $60 \times Ta_2O_5 + 50 \times TiO_2 + 60 \times Ta_2O_5$ ALD cycles, denoting the consequent numbers of the constituent oxide growth cycles. The second three-layer structures were TiO_2-Ta_2O_5-TiO_2 stacks, with an ALD sequence of $50 \times TiO_2 + 70 \times Ta_2O_5 + 50 \times TiO_2$ ALD cycles. Additional TiO_2 films embedding a monolayer of Ta_2O_5 were also grown after $75 \times TiO_2 + 3 \times Ta_2O_5 + 75 \times TiO_2$, and $75 \times TiO_2 + 1 \times Ta_2O_5 + 75 \times TiO_2$ ALD cycles. Hereafter, the above mentioned stacked films will be denoted as samples TL1, TL2, EL3 and EL1, respectively (see Table I). Top electrodes were Pt dots with two different areas (0.52×10^{-3} cm^2 and 2.04×10^{-3} cm^2).

The phase composition of the films structure was evaluated from X-ray diffraction analyses (XRD). X-Ray measurements were performed at room temperature on a materials research X-ray diffractometer SmartLab (Rigaku™) using CuKα radiation from a 9 kW rotating anode. The pure Ta_2O_5 film exhibited a crystal structure, but all mixed films of Ta_2O_5 and TiO_2 were amorphous (Fig. 1). Short-range order was recognized, however, in the EL1 film in which only one monolayer of Ta_2O_5 was deposited between two TiO_2 layers. In the Raman spectra of the EL1 sample (Fig. 2), a peak typical for anatase phase was detected at 143-145 cm^{-1} [16, 17], also seen earlier in TiO_2 films grown by ALD from $TiCl_4$ and H_2O [12]. In the EL3 sample, three Ta_2O_5 growth cycles were applied between the halves of the TiO_2 host layer, and the structural disorder was evidently increased.

Consequently, anatase phase could not be recognized any more. Instead, broad Raman bands appeared at 300 and 800 cm^{-1}, which cannot be attributed to any known TiO_2 phase, neither can any band in this spectrum be regarded as that characteristic of ruthenium oxide electrode substrate [18]. In summary, the films studied are essentially amorphous and highly defective, as is confirmed from scanning electron microscopy (SEM) micrographs (Fig. 3). We have not applied any post deposition heat treatment to prevent film crystallization and, consequently, dielectric degradation.

ELECTRICAL CHARACTERIZATION AND DISCUSSION

Electrical measurements of MIM structures were carried out putting the sample in a light-proof, electrically shielded box. Samples were electrically characterized in both d.c. and a.c. regimes using a Keithley 4200SCS semiconductor analyzer. The conductive filaments were electroformed by DC bias sweeping from 0 to 0.7 V with a current compliance of 10 mA. Then, successive low-resistance state (LRS) to high-resistance state (HRS) I-V cycles were recorded with current compliance of 100 mA. For the small signal study of the devices, the real (G) and imaginary (B) components of the admittance were measured as functions of the dc voltage bias with a superimposed 30 mV rms signal at a frequency of 100 kHz.

Fig. 3 shows 50 successive I-V resistive switching cycles of a TL1 MIM sample at room temperature. Voltage bias applied was progressively varied as indicated by arrows. Positive voltages induce the transition to the low resistance state (set) at a voltage of about 0.6 V. The transition to the high resistance state occurs at reset voltages of about -0.8 V. The most likely hypothesis for the resistive switching is the generation of oxygen vacancies under the applied electric field during positive voltage sweep [19]. Oxygen vacancies tend to cluster and generally form filamentary shapes under an electric field. When such clusters are formed, the resistance of the local region becomes much lower than that of the surrounding oxide, and the low and high resistance states are determined by the creation and rupture of the conductive filaments.

All samples in this study exhibited bipolar resistive switching, but noticeable differences have been observed. In Fig. 4, I-V loops for the four devices studied in this work are plotted. The three-layers samples (TL1 and TL2) have similar I-V loops, regardless the dielectric film ordering. In contrast, TiO_2 films embedding a monolayer of Ta_2O_5 (EL3 and EL1) show different loops. The sample with monolayer of Ta_2O_5 grown after 3 ALD cycles (EL3) exhibits the lowest values of the current, i.e., the least power consumption at both states.

resistance state. However, it provides small differences between the current at the ON and the OFF state. The sample with the thinnest monolayer of Ta_2O_5 (EL1) exhibits the best performance. The difference between the current in the ON and the OFF state is the highest, and the currents at the LRS and HRS states are lower than in the three-layer samples. Small signal ac parameters also show hysteretic behavior during the whole bipolar switching cycle. The real (G) and imaginary (B) parts of the three-layer (TL1) and an embedded monolayer (EL1) samples are plotted in Fig. 5. Noticeable differences can be recognized. The three-layer sample shows two well differentiated values in the ON and OFF states. At the OFF state, the conductance has lower values and increases at positive voltages until reaching the ON state. When the sample is at the ON state, G remains nearly constant at voltage values higher than the reset voltage. When the ON to OFF switching occurs (Reset), the conductance experiences a quick increase. The imaginary part (susceptance, B) is high at the OFF state, and gradually decreases towards the set voltage. At the ON state, B remains constant and suddenly decreases when the reset occurs, and becomes negative for voltages beyond -1 V. Negative values of susceptance reveal an inductive-like behavior. In contrast, the sample with an embedded monolayer exhibits loops in which the differences between the ON and OFF states are more moderate, G and B monotonically vary with the voltage without sudden increment or decrement at the reset transition.

These results indicate that the conductive filaments in samples consisting of 3 layers with a thickness of about 1.7 nm each must be very different from those possibly formed in the stack consisting of a TiO_2 film embedding very thin (1-3 ALD cycles only) Ta_2O_5 monolayer. In the first case, resistive switching requires the formation of conductive filaments in all tree layers. Therefore, electroforming must occur in all TiO_2 and Ta_2O_5 layers, regardless the material ordering. When a monolayer of Ta_2O_5 is embedded between two thicker TiO_2 layers, it is possible to obtain resistive switching when only the TiO_2 films are electroformed. In this case a discontinuity in the filaments may occur at the Ta_2O_5 monolayer. But, because this discontinuity is very thin, electron tunneling can occur through it, allowing d.c. currents between the top and bottom electrodes. That can explain why the currents are lower in the sample containing 3 cycles monolayer (EL3) compared to those in the sample containing 1 cycle monolayer (EL1) - thinner monolayer enables more effective tunneling.

Conductive filaments consist of a continuum of oxygen vacancy, V_O, clusters. When a negative voltage is applied, oxygen ions can migrate toward the bottom electrode and occupy vacancy sites. Consequently, discontinuities in the oxygen vacancy clusters appear and the conductive filaments are interrupted, and the high-resistance state is restored. As for the small signal response, the oxygen ion displacement adds new terms to the

real and imaginary part of the admittance. The conductive term, *G*, is increased by the oxygen ions flowing through oxygen vacancies in the conductive filament. Time delays between the oxygen ions response and the applied a.c. voltage are responsible for the appearance of a negative term in the imaginary part of the admittance, *B*. In the case of EL samples, the embedded layer prevents the oxygen ions passage through. As a result, oxygen ions are trapped in this very defective monolayer and do not give rise to the artefacts observed in the admittance curves of TL type samples, and the variations of *G* and *B* are much more moderate in EL samples than in those of the type TL.

SUMMARY

Two types of 5 nm-thick metal-insulator-metal devices consisting on Ta_2O_5-TiO_2-Ta_2O_5 and TiO_2-Ta_2O_5-TiO_2 stacks on 15 nm-RuO2/10 nm-TiN/Si substrates have been fabricated by ALD: three-layer films of Ta_2O_5-TiO_2-Ta_2O_5 and TiO_2-Ta_2O_5-TiO_2 (TL1 and TL2) stacks with similar thickness of all layers (about 1.7 nm) and TiO_2 films embedding a monolayer of 1 and 3 ALD cycles of Ta_2O_5 (EL1 and EL3). XRD and Raman analysis reveal that the films studied are essentially amorphous and highly defective. This microscopic nature causes that all samples exhibit bipolar resistive switching behavior, and makes these devices potentially suitable for RRAM memory application. The best behavior is obtained for samples with one monolayer of 1 ALD cycle of Ta_2O_5 embedded in a total thickness of 5 nm or TiO_2: the highest ON to OFF current ratio, and lower current levels at the LRS and HRS states are lower than in the three-layer samples, TL1 and TL2. Admittance measurements reveal significant differences between the two types of samples as well. The three-layer samples show two well differentiated values at the ON and OFF states, and very sharped changes during the ON to OFF state transition (reset) on both in-phase (conductance) and in-quadrature (susceptance) components. In contrast, more gradual and narrower loops are obtained for samples with an embedded monolayer. Sharp changes during the reset cycle are not observed in these samples. These differences were explained as due to a different nature for the conductive filaments causing the resistive switching behavior. Conductive paths are attributed to clusters of oxygen vacancy defects. In the case of three-layer samples electroforming must occur in all TiO_2 and Ta_2O_5 layers, regardless the material ordering. In the case of samples EL1 and EL3, a discontinuity in the filaments occurs at the Ta_2O_5 monolayer. This discontinuity is thin enough to allow tunneling of electrons flowing between the device electrodes. Finally, oxygen ions are trapped in this very defective monolayer and do not give rise to the sharp variations observed in the admittance curves of TL-type samples.

Acknowledgements

This work was funded by the Spanish Ministry of Economy and Competitiveness through project TEC2014-52152-C3-3-R, with support of Feder funds, Estonian Research Agency (PUT170, IUT2-24), and by the European Regional Development Fund projects TK134 and TK141.

REFERENCES

[1] A. Beck, J. G. Bednorz, C. Gerber, C. Rossel, and D. Widmer, Appl. Phys. Lett. 77(1), 139 (2000).

[2] R. Waser and M. Aono, Nature Mater. 6 (11), 833 (2007).

[3] J.J. Yang, D.B. Strukov, D.R. Stewart, Nat.Nanotechnol. 8, 13 (2013).

[4] E. Gale, Semicond. Sci. Technol. 29, 104004 (2014).

[5] H. Nili, S. Walia, S. Balendhran, D.B. Strukov, M. Bhaskaran, S. Sriram, Adv. Funct. Mater. 24, 6741 (2014)

[6] C. Chen, Y.C. Yang, F. Zeng, F. Pan, Appl. Phys. Lett. 97, 083502 (2010)

[7] Y.-T. Huang, C.-W. Huang, J.-Y. Chen, Y.-H. Ting, K.-C. Lu, Y.-L. Chueh, and W.-W.Wu., ACS Nano 8, 9457 (2014).

[8]. R. Waser, R. Bruchhaus, and S. Menzel, in Nanoelectronics and Information Technology. Advanced Electronic Materials and Novel Devices, ed. By R. Waser and P. Grumberg (Wiley-VCH, Germany 2012), p. 683.

[9] J. Yoon, H. Choi, D. Lee, J. B. Park, J. Lee, D. J. Seong, Y. Ju, M. Chang, S. Jung, and H. Hwang, IEEE Electron Device Lett. 30 (5), p. 457 (2009).

[10] M. H. Lin, M. C. Wu, C. Y. Huang, C. Y. Huang, C. H. Lin, and T. Y. Tseng, J. Phys. D, Appl. Phys. 43(29), p. 295404 (2010).

[11] C. H. Cheng, A. Chin, and F. S. Yeh, IEEE Electron Device Lett.31(9), p. 1020 (2010).

[12] M. Terai, Y. Sakotsubo, S. Kotsuji, and H. Hada IEEE Electron Device Lett. 31 (3), p. 204 (2010).

[13] M. J. Kim, I. G. Baek, Y. H. Ha, S. J. Baik, J. H. Kim, D. J. Seong, S. J. Kim, Y. H. Kwon, C. R. Lim, H. K. Park, D. Gilmer, P. Kirsch, R. Jammy, Y. G. Shin, S. Choi, and C. Chung, IEDM Tech. Dig. 2010, p444 (2010).

[14] Y.L. Song, Y. Liu, Y.L. Wang, X.P. Tian, L.M. Yang, Y.Y. Lin, IEEE Electron Device Lett. 32, p. 1439 (2011)

[15] T. Arroval, L. Aarik, R. Rammula, V. Kruusla, and J. Aarik, Thin Solid Films 600, 119 (2016).

[16] B. Karunagaran, K. Kim, D. Mangalaraj, J. Yi, and S. Velumani, Solar Energy Materials & Solar Cells 88, 199 (2005).

[17] O. Frank, M. Zukalova, B. Laskova, J. Kürti, J Koltai, and L. Kavan, Phys. Chem. Chem. Phys. 14, 14567 (2012).

[18] S. Bhaskar, P. S. Dobal, S. B. Majumder, and R. S. Katiyar, J. Appl. Phys. 89, 2987, 2001.

[19] B. Hudec, A. Paskaleva, P. Jancovic, J. Dérer, J. Fedor A. Rosová, E. Dobrocka, and K. Fröhlich, Thin Solid Films, 563, 10 (2014).

Table I. Dielectric films description

Sample	ALD cycles	Thickness (nm)
TL1	60 xTa_2O_5 + 50 xTiO_2 + 60xTa_2O_5	4.0 nm
TL2	50 xTiO_2 + 70 xTa_2O_5 + 50x TiO_2	4.0 nm
EL3	75 xTiO_2 + 3 xTa_2O_5 + 75x TiO_2	5.5. nm
EL1	75 xTiO_2 + 1 xTa_2O_5 + 75x TiO_2	5.0 nm

FIGURE CAPTIONS

FIG.1. XRD diffraction spectra of TL1, TL2, EL1 and EL3 samples. (A film of pure Ta_2O_5 has be included for reference).

FIG.2. Raman spectroscopy results obtained for samples EL1 and EL3.

FIG. 3. SEM micrographs of samples TL1 (a), TL2 (b), EL1(c) and EL3 (d).

FIG. 4. 50 successive cycles of I-V bipolar resistive switching obtained for a 5nm Ta_2O_5-TiO_2-Ta_2O_5 stack.

FIG. 5. Comparative of the I-V resistive switching loops for the samples in this study.

FIG. 6. G-V (a) and B/ω (b) as a function of the bias voltage during a resistive switching loops for EL1 and TL1 sample.

Manuscript
Click here to view linked References
Click here to download Manuscript Duenas_DRIP17_revised.pdf

1
2
3
4
5
6
7
8
9
10
11
12
13
14
15
16
17
18
19
20
21
22
23
24
25
26
27
28
29
30
31
32
33
34
35
36
37
38
39
40
41
42
43
44
45
46
47
48
49
50
51
52
53
54
55
56
57
58
59
60
61
62
63
64
65

The role of defects on the resistive switching behavior of Ta_2O_5-TiO_2 based metal-insulator-metal (MIM) devices for memory applications

S. DUEÑAS[1,4], H. CASTÁN[1], H. GARCÍA[1], O. G. OSSORIO[1], L. A. DOMÍNGUEZ[1],

H. SEEMEN[2], A. TAMM[2], K. KUKLI[2,3], and J. AARIK[2]

1.- Department of Electronics, University of Valladolid, Campus Miguel Delibes, 47011 Valladolid, Spain

2.- Institute of Physics, University of Tartu, W. Ostwald 1, 50411 Tartu, Estonia

3.- Department of Chemistry, University of Helsinki, P.O. Box 55, FI-00014 Helsinki, Finland

4.- e-mail: sduenas@ele.uva.es

ABSTRACT

In this work we describe the role of defects on the resistive switching behavior of metal-insulator-metal devices based on alternating Ta_2O_5 and TiO_2 stacks. Ruthenium oxide, RuO_x, and platinum, Pt, were used as bottom and top electrodes, respectively. 5 nm-thick insulator stacks were fabricated by atomic layer deposition of alternating Ta_2O_5 and TiO_2 thin films. Bipolar resistive switching behavior was obtained on Ta_2O_5-TiO_2-Ta_2O_5 and TiO_2-Ta_2O_5-TiO_2 stacks. These behavior is mainly due to the presence of oxygen vacancy defects. The best memristive response was obtained in the case of two TiO_2 films embedding a monolayer of Ta_2O_5. Very repetitive direct current (dc) - voltage bipolar switching cycles were obtained. Small signal admittance parameters also showed hysteretic behavior during a whole bipolar switching cycle. In the case of samples with three layers of similar thickness, when the transition from the ON to the OFF state (Reset) occurs, the conductance abruptly increases and the susceptance experiences fast decreasing for more negative voltages values. Such behavior was not observed when only one Ta_2O_5 monolayer was examined. These differences are explained in terms of charge transport mechanism occurring in the open conductive filaments.

KEY WORDS: Resistive switching, tantalum oxide, titanium oxide, defects, metal-insulator-metal, high-k dielectric stacks.

INTRODUCTION

Resistive random-access memories (RRAM) are nowadays very well reputed challengers to fabricate low power, high density and high endurance nonvolatile memories (NVM) [1-2]. An additional advantage of RRAMs is the possibility to become fabricated as three-dimensional cross bar arrays (CBA). They are based on the memristive properties of various insulators, including binary oxides, perovskites, nitrides and selenides [3-7]. RRAMs working principle is based on the reversible formation and rupture of single or multiple nanoconfined conductive filaments (CF) between the two electrodes of a metal-insulator-metal (MIM) or metal-insulator-semiconductor (MIS) structure. The conductive filaments are formed by the accumulation of defects (metallic atoms, or oxygen vacancies, for instance) throughout the insulator. Based on the nature of the defects and the principal operation mechanisms of resistive switching, different kind of RRAMs can be obtained: valence change memory (VCM), electrochemical metallization memory (ECM), or thermochemical memory (TCM). The VCM memories are based on redox reactions which yield the creation and migration of oxygen vacancies through networks of defects and change the conductivity. This mechanism usually produces bipolar switching devices. ECM and TCM memories are based on the combination of redox reactions and Joule heating in the filament and its neighboring regions. Metallic filaments are created during the electroforming and are interrupted by electric field assisted Joule heating during the Reset pulse. Subsequent Joule heating-assisted reduction of the interrupted filament rebuilds the filament so switching the device to the conductive state (Set). Both mechanisms can be achieved with the same bias polarity (unipolar switching behavior).

During the last decade a variety of high permittivity oxides, e.g. HfO_2, ZrO_2, TiO_2, Ta_2O_5, $SrTiO_3$, NiO, have been proposed as challengers for resistive switching [8]. To reach an accurate control of RRAM devices, an in-depth knowledge about the role and density of defects on the CF formation and dilution is mandatory. Moreover, the potential applications of high-k based RRAMs requires a careful design of the switching layer structure to obtain RRAM devices with excellent performance and reliability. Due to the expected high density of RRAMs, low power consumption and good uniformity must be warranted. To reduce power consumption, several methods have been proposed, such as using bilayer structure and device area scaling [9-13]. The bilayer structure is considered as the most promising approach, and the improved characteristics of these bilayer devices are displayed adequately [11,12]. Some high-k dielectrics exhibit good resistive switching behavior. Others are not so good in terms of switching, but are better in terms of leakage current and thermodynamic stability. The combination of materials having complementary properties is the key for the interest in bilayer structures [14].

In this work, resistive switching phenomena on Ta_2O_5 and TiO_2 multilayers based metal-insulator-metal (MIM) structures are reported. Ta_2O_5-TiO_2 films were grown to target thickness of 5 nm. The films were grown either as multilayer stacks of Ta_2O_5 and TiO_2 or TiO_2 films embedding a monolayer of Ta_2O_5. The stacks were grown to stabilize the conductive filaments in TiO_2 by inserting otherwise more insulating tantalum oxide, and examine the possible effect of layering different metal oxides on the resulting RRAM devices.

SAMPLE DESCRIPTION

MIM samples were obtained by depositing the films on 15 nm-RuO_2/10 nm-TiN/Si substrates. Oxide films were grown in an in-house built low-pressure flow-type atomic-layer-deposition (ALD) reactor [15, 16] in the form of stacks consisting of TiO_2-Ta_2O_5-TiO_2 or Ta_2O_5-TiO_2-Ta_2O_5 triple layers at the substrate temperature of 350 ºC. Metal chloride precursors, $TiCl_4$ and $TaCl_5$, were used to grow TiO_2 and Ta_2O_5, respectively. Ozone was used as oxygen precursor. TiO_2 layers were grown using cycle times 2-2-5-5 s, denoting sequence of $TiCl_4$ pulse length – purge time - ozone pulse length - purge time, respectively. For Ta_2O_5, the corresponding cycle times were 3-2-5-5 s. Four different multilayer structures of alternating Ta_2O_5 and TiO_2 were fabricated. First, a three-layer Ta_2O_5-TiO_2-Ta_2O_5 were fabricated with a sequence of $60 \times Ta_2O_5 + 50 \times TiO_2 + 60 \times Ta_2O_5$ ALD cycles, denoting the consequent numbers of the constituent oxide growth cycles. The second three-layer structures were TiO_2-Ta_2O_5-TiO_2 stacks, with an ALD sequence of $50 \times TiO_2 + 70 \times Ta_2O_5 + 50 \times TiO_2$ ALD cycles. Additional TiO_2 films embedding a monolayer of Ta_2O_5 were also grown after $75 \times TiO_2 + 3 \times Ta_2O_5 + 75 \times TiO_2$, and $75 \times TiO_2 + 1 \times Ta_2O_5 + 75 \times TiO_2$ ALD cycles. Hereafter, the above mentioned stacked films will be denoted as samples TL1, TL2, EL3 and EL1, respectively (see Table I). Top electrodes were Pt dots with two different areas (0.52×10^{-3} cm^2 and 2.04×10^{-3} cm^2).

The phase composition of the films structure was evaluated from X-ray diffraction analyses (XRD). X-Ray measurements were performed at room temperature on a materials research X-ray diffractometer SmartLab (Rigaku™) using CuKα radiation from a 9 kW rotating anode. The pure Ta_2O_5 film exhibited a crystal structure, but all mixed films of Ta_2O_5 and TiO_2 were amorphous (Fig. 1). Short-range order was recognized, however, in the EL1 film in which only one monolayer of Ta_2O_5 was deposited between two TiO_2 layers. In the Raman spectra of the EL1 sample (Fig. 2), a peak typical for anatase phase was detected at 143-145 cm^{-1} [16, 17], also seen earlier in TiO_2 films grown by ALD from $TiCl_4$ and H_2O [12]. In the EL3 sample, three Ta_2O_5 growth cycles were applied between the halves of the TiO_2 host layer, and the structural disorder was evidently increased.

Consequently, anatase phase could not be recognized any more. Instead, broad Raman bands appeared at 300 and 800 cm^{-1}, which cannot be attributed to any known TiO_2 phase, neither can any band in this spectrum be regarded as that characteristic of ruthenium oxide electrode substrate [18]. In summary, the films studied are essentially amorphous and highly defective, as is confirmed from scanning electron microscopy (SEM) micrographs (Fig. 3). We have not applied any post deposition heat treatment to prevent film crystallization and, consequently, dielectric degradation.

ELECTRICAL CHARACTERIZATION AND DISCUSSION

Electrical measurements of MIM structures were carried out putting the sample in a light-proof, electrically shielded box. Samples were electrically characterized in both d.c. and a.c. regimes using a Keithley 4200SCS semiconductor analyzer. The conductive filaments were electroformed by DC bias sweeping from 0 to 0.7 V with a current compliance of 10 mA. Then, successive low-resistance state (LRS) to high-resistance state (HRS) I-V cycles were recorded with current compliance of 100 mA. For the small signal study of the devices, the real (G) and imaginary (B) components of the admittance were measured as functions of the dc voltage bias with a superimposed 30 mV rms signal at a frequency of 100 kHz.

Fig. 3 shows 50 successive I-V resistive switching cycles of a TL1 MIM sample at room temperature. Voltage bias applied was progressively varied as indicated by arrows. Positive voltages induce the transition to the low resistance state (set) at a voltage of about 0.6 V. The transition to the high resistance state occurs at reset voltages of about -0.8 V. The most likely hypothesis for the resistive switching is the generation of oxygen vacancies under the applied electric field during positive voltage sweep [19]. Oxygen vacancies tend to cluster and generally form filamentary shapes under an electric field. When such clusters are formed, the resistance of the local region becomes much lower than that of the surrounding oxide, and the low and high resistance states are determined by the creation and rupture of the conductive filaments.

All samples in this study exhibited bipolar resistive switching, but noticeable differences have been observed. In Fig. 4, I-V loops for the four devices studied in this work are plotted. The three-layers samples (TL1 and TL2) have similar I-V loops, regardless the dielectric film ordering. In contrast, TiO_2 films embedding a monolayer of Ta_2O_5 (EL3 and EL1) show different loops. The sample with monolayer of Ta_2O_5 grown after 3 ALD cycles (EL3) exhibits the lowest values of the current, i.e., the least power consumption at both states.

resistance state. However, it provides small differences between the current at the ON and the OFF state. The sample with the thinnest monolayer of Ta_2O_5 (EL1) exhibits the best performance. The difference between the current in the ON and the OFF state is the highest, and the currents at the LRS and HRS states are lower than in the three-layer samples. Small signal ac parameters also show hysteretic behavior during the whole bipolar switching cycle. The real (G) and imaginary (B) parts of the three-layer (TL1) and an embedded monolayer (EL1) samples are plotted in Fig. 5. Noticeable differences can be recognized. The three-layer sample shows two well differentiated values in the ON and OFF states. At the OFF state, the conductance has lower values and increases at positive voltages until reaching the ON state. When the sample is at the ON state, G remains nearly constant at voltage values higher than the reset voltage. When the ON to OFF switching occurs (Reset), the conductance experiences a quick increase. The imaginary part (susceptance, B) is high at the OFF state, and gradually decreases towards the set voltage. At the ON state, B remains constant and suddenly decreases when the reset occurs, and becomes negative for voltages beyond -1 V. Negative values of susceptance reveal an inductive-like behavior. In contrast, the sample with an embedded monolayer exhibits loops in which the differences between the ON and OFF states are more moderate, G and B monotonically vary with the voltage without sudden increment or decrement at the reset transition.

These results indicate that the conductive filaments in samples consisting of 3 layers with a thickness of about 1.7 nm each must be very different from those possibly formed in the stack consisting of a TiO_2 film embedding very thin (1-3 ALD cycles only) Ta_2O_5 monolayer. In the first case, resistive switching requires the formation of conductive filaments in all tree layers. Therefore, electroforming must occur in all TiO_2 and Ta_2O_5 layers, regardless the material ordering. When a monolayer of Ta_2O_5 is embedded between two thicker TiO_2 layers, it is possible to obtain resistive switching when only the TiO_2 films are electroformed. In this case a discontinuity in the filaments may occur at the Ta_2O_5 monolayer. But, because this discontinuity is very thin, electron tunneling can occur through it, allowing d.c. currents between the top and bottom electrodes. That can explain why the currents are lower in the sample containing 3 cycles monolayer (EL3) compared to those in the sample containing 1 cycle monolayer (EL1) - thinner monolayer enables more effective tunneling.

Conductive filaments consist of a continuum of oxygen vacancy, V_O, clusters. When a negative voltage is applied, oxygen ions can migrate toward the bottom electrode and occupy vacancy sites. Consequently, discontinuities in the oxygen vacancy clusters appear and the conductive filaments are interrupted, and the high-resistance state is restored. As for the small signal response, the oxygen ion displacement adds new terms to the

real and imaginary part of the admittance. The conductive term, *G*, is increased by the oxygen ions flowing through oxygen vacancies in the conductive filament. Time delays between the oxygen ions response and the applied a.c. voltage are responsible for the appearance of a negative term in the imaginary part of the admittance, *B*. In the case of EL samples, the embedded layer prevents the oxygen ions passage through. As a result, oxygen ions are trapped in this very defective monolayer and do not give rise to the artefacts observed in the admittance curves of TL type samples, and the variations of *G* and *B* are much more moderate in EL samples than in those of the type TL.

SUMMARY

Two types of 5 nm-thick metal-insulator-metal devices consisting on Ta_2O_5-TiO_2-Ta_2O_5 and TiO_2-Ta_2O_5-TiO_2 stacks on 15 nm-RuO2/10 nm-TiN/Si substrates have been fabricated by ALD: three-layer films of Ta_2O_5-TiO_2-Ta_2O_5 and TiO_2-Ta_2O_5-TiO_2 (TL1 and TL2) stacks with similar thickness of all layers (about 1.7 nm) and TiO_2 films embedding a monolayer of 1 and 3 ALD cycles of Ta_2O_5 (EL1 and EL3). XRD and Raman analysis reveal that the films studied are essentially amorphous and highly defective. This microscopic nature causes that all samples exhibit bipolar resistive switching behavior, and makes these devices potentially suitable for RRAM memory application. The best behavior is obtained for samples with one monolayer of 1 ALD cycle of Ta_2O_5 embedded in a total thickness of 5 nm or TiO_2: the highest ON to OFF current ratio, and lower current levels at the LRS and HRS states are lower than in the three-layer samples, TL1 and TL2. Admittance measurements reveal significant differences between the two types of samples as well. The three-layer samples show two well differentiated values at the ON and OFF states, and very sharped changes during the ON to OFF state transition (reset) on both in-phase (conductance) and in-quadrature (susceptance) components. In contrast, more gradual and narrower loops are obtained for samples with an embedded monolayer. Sharp changes during the reset cycle are not observed in these samples. These differences were explained as due to a different nature for the conductive filaments causing the resistive switching behavior. Conductive paths are attributed to clusters of oxygen vacancy defects. In the case of three-layer samples electroforming must occur in all TiO_2 and Ta_2O_5 layers, regardless the material ordering. In the case of samples EL1 and EL3, a discontinuity in the filaments occurs at the Ta_2O_5 monolayer. This discontinuity is thin enough to allow tunneling of electrons flowing between the device electrodes. Finally, oxygen ions are trapped in this very defective monolayer and do not give rise to the sharp variations observed in the admittance curves of TL-type samples.

Acknowledgements

This work was funded by the Spanish Ministry of Economy and Competitiveness through project TEC2014-52152-C3-3-R, with support of Feder funds, Estonian Research Agency (PUT170, IUT2-24), and by the European Regional Development Fund projects TK134 and TK141.

REFERENCES

[1] A. Beck, J. G. Bednorz, C. Gerber, C. Rossel, and D. Widmer, Appl. Phys. Lett. 77(1), 139 (2000).

[2] R. Waser and M. Aono, Nature Mater. 6 (11), 833 (2007).

[3] J.J. Yang, D.B. Strukov, D.R. Stewart, Nat.Nanotechnol. 8, 13 (2013).

[4] E. Gale, Semicond. Sci. Technol. 29, 104004 (2014).

[5] H. Nili, S. Walia, S. Balendhran, D.B. Strukov, M. Bhaskaran, S. Sriram, Adv. Funct. Mater. 24, 6741 (2014)

[6] C. Chen, Y.C. Yang, F. Zeng, F. Pan, Appl. Phys. Lett. 97, 083502 (2010)

[7] Y.-T. Huang, C.-W. Huang, J.-Y. Chen, Y.-H. Ting, K.-C. Lu, Y.-L. Chueh, and W.-W.Wu., ACS Nano 8, 9457 (2014).

[8]. R. Waser, R. Bruchhaus, and S. Menzel, in Nanoelectronics and Information Technology. Advanced Electronic Materials and Novel Devices, ed. By R. Waser and P. Grumberg (Wiley-VCH, Germany 2012), p. 683.

[9] J. Yoon, H. Choi, D. Lee, J. B. Park, J. Lee, D. J. Seong, Y. Ju, M. Chang, S. Jung, and H. Hwang, IEEE Electron Device Lett. 30 (5), p. 457 (2009).

[10] M. H. Lin, M. C. Wu, C. Y. Huang, C. Y. Huang, C. H. Lin, and T. Y. Tseng, J. Phys. D, Appl. Phys. 43(29), p. 295404 (2010).

[11] C. H. Cheng, A. Chin, and F. S. Yeh, IEEE Electron Device Lett.31(9), p. 1020 (2010).

[12] M. Terai, Y. Sakotsubo, S. Kotsuji, and H. Hada IEEE Electron Device Lett. 31 (3), p. 204 (2010).

[13] M. J. Kim, I. G. Baek, Y. H. Ha, S. J. Baik, J. H. Kim, D. J. Seong, S. J. Kim, Y. H. Kwon, C. R. Lim, H. K. Park, D. Gilmer, P. Kirsch, R. Jammy, Y. G. Shin, S. Choi, and C. Chung, IEDM Tech. Dig. 2010, p444 (2010).

[14] Y.L. Song, Y. Liu, Y.L. Wang, X.P. Tian, L.M. Yang, Y.Y. Lin, IEEE Electron Device Lett. 32, p. 1439 (2011)

[15] T. Arroval, L. Aarik, R. Rammula, V. Kruusla, and J. Aarik, Thin Solid Films 600, 119 (2016).

[16] B. Karunagaran, K. Kim, D. Mangalaraj, J. Yi, and S. Velumani, Solar Energy Materials & Solar Cells 88, 199 (2005).

[17] O. Frank, M. Zukalova, B. Laskova, J. Kürti, J Koltai, and L. Kavan, Phys. Chem. Chem. Phys. 14, 14567 (2012).

[18] S. Bhaskar, P. S. Dobal, S. B. Majumder, and R. S. Katiyar, J. Appl. Phys. 89, 2987, 2001.

[19] B. Hudec, A. Paskaleva, P. Jancovic, J. Dérer, J. Fedor A. Rosová, E. Dobrocka, and K. Fröhlich, Thin Solid Films, 563, 10 (2014).

Table I. Dielectric films description

Sample	ALD cycles	Thickness (nm)
TL1	60 xTa_2O_5 + 50 $xTiO_2$ + 60xTa_2O_5	4.0 nm
TL2	50 $xTiO_2$ + 70 xTa_2O_5 + 50x TiO_2	4.0 nm
EL3	75 $xTiO_2$ + 3 xTa_2O_5 + 75x TiO_2	5.5. nm
EL1	75 $xTiO_2$ + 1 xTa_2O_5 + 75x TiO_2	5.0 nm

FIGURE CAPTIONS

FIG.1. XRD diffraction spectra of TL1, TL2, EL1 and EL3 samples. (A film of pure Ta_2O_5 has be included for reference).

FIG.2. Raman spectroscopy results obtained for samples EL1 and EL3.

FIG. 3. SEM micrographs of samples TL1 (a), TL2 (b), EL1(c) and EL3 (d).

FIG. 4. 50 successive cycles of I-V bipolar resistive switching obtained for a 5nm Ta_2O_5-TiO_2-Ta_2O_5 stack.

FIG. 5. Comparative of the I-V resistive switching loops for the samples in this study.

FIG. 6. G-V (a) and B/ω (b) as a function of the bias voltage during a resistive switching loops for EL1 and TL1 sample.

Figure 1

Click here to download Figure Fig1.jpg

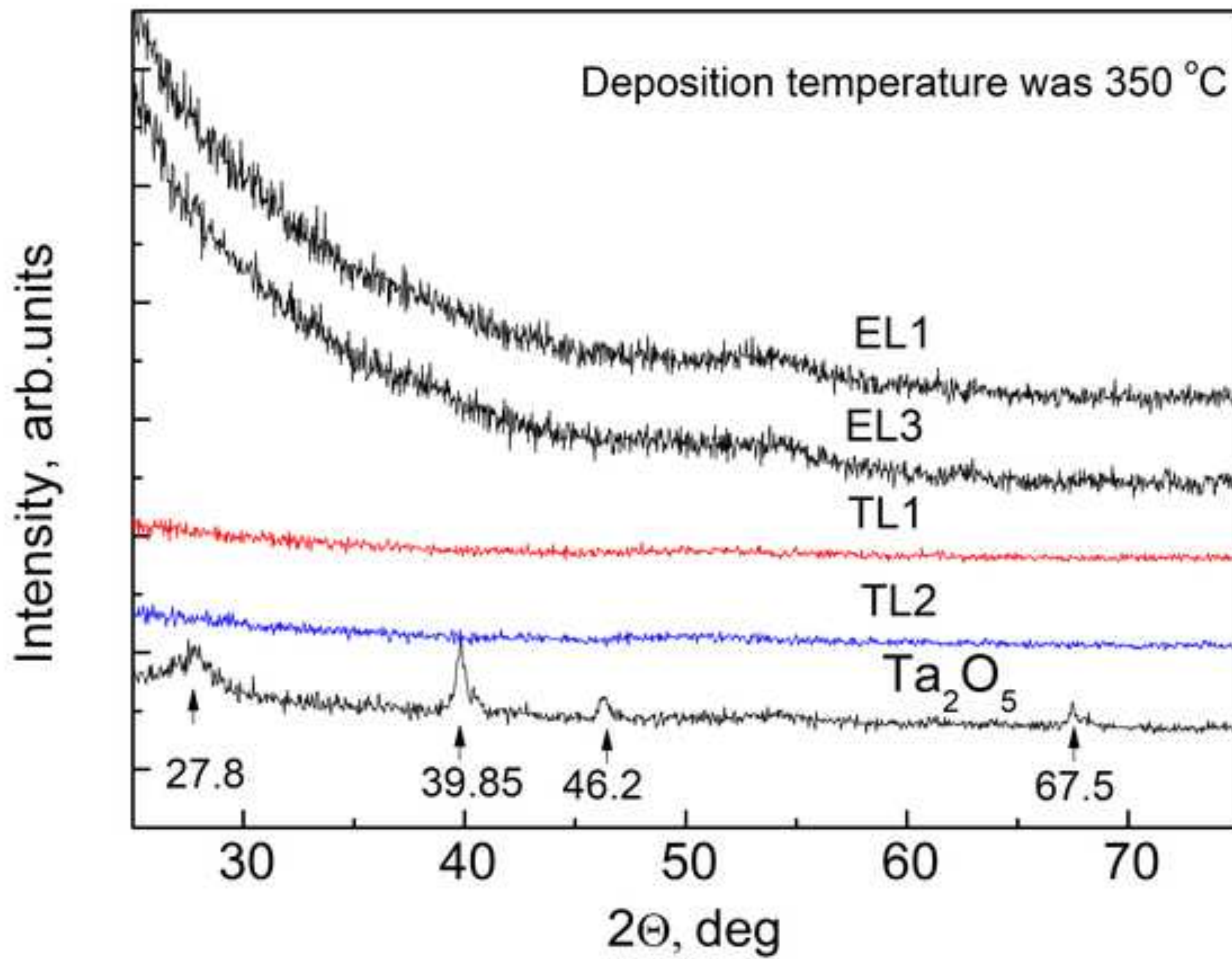

Figure 2

Click here to download Figure Fig2.jpg

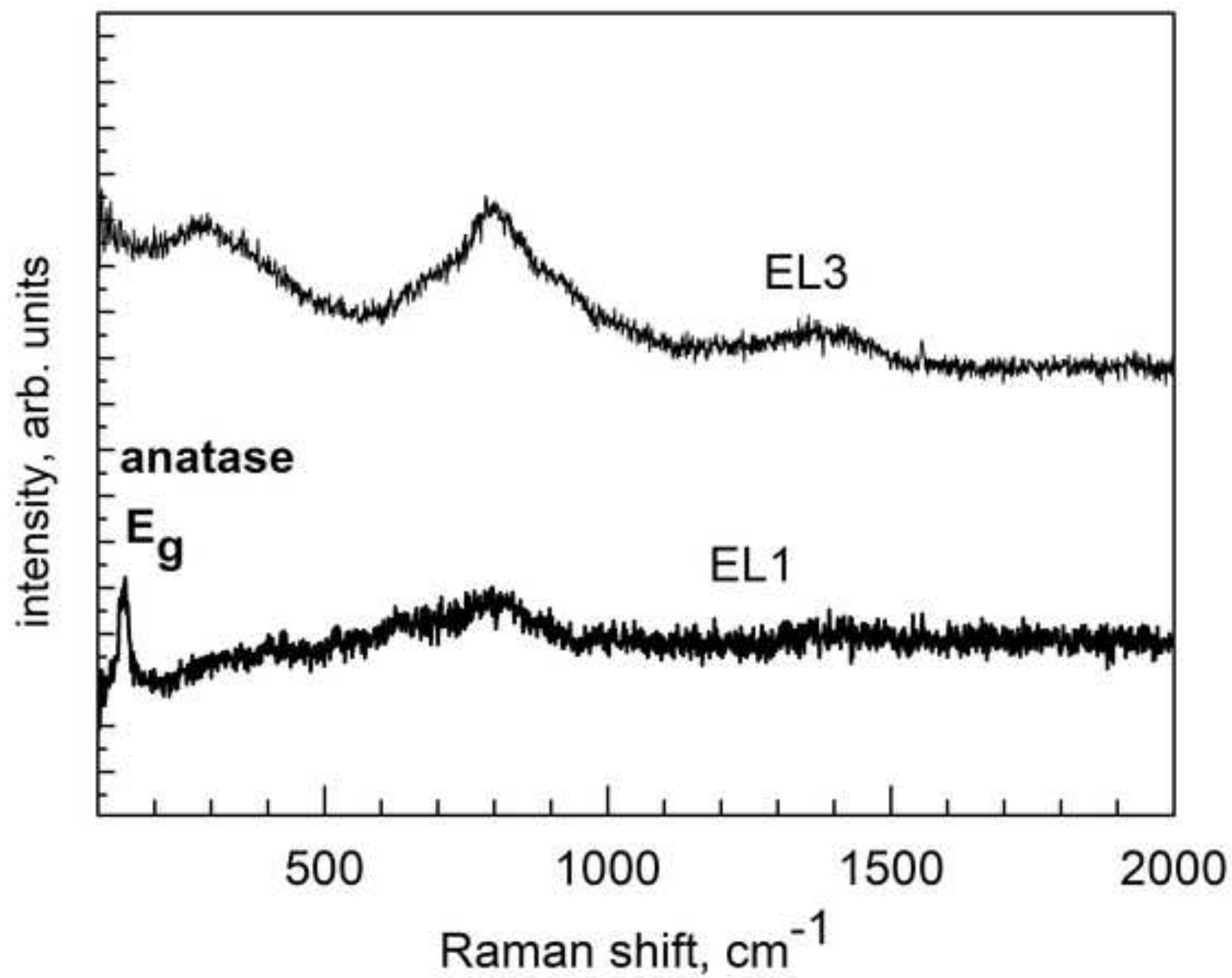

Figure 3

Click here to download Figure Fig3.jpg

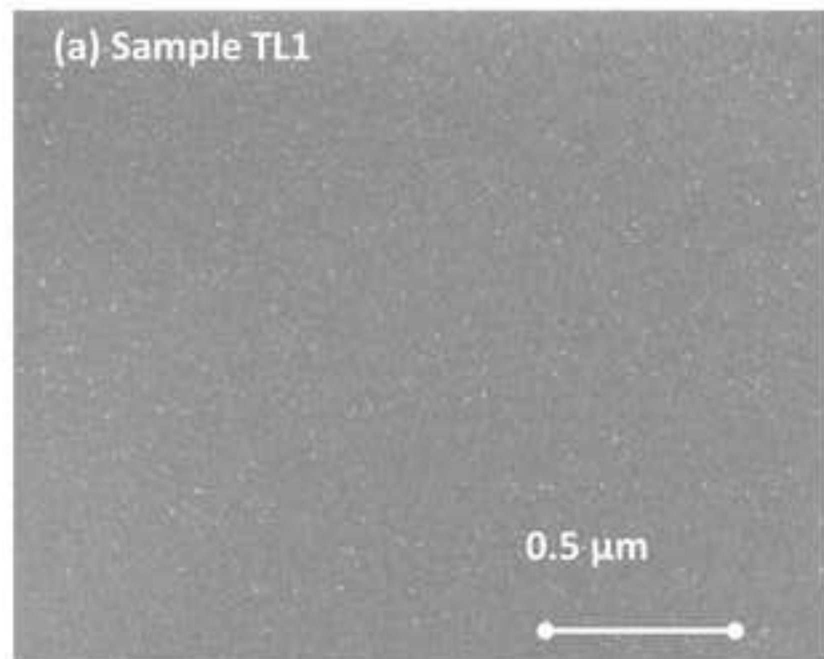

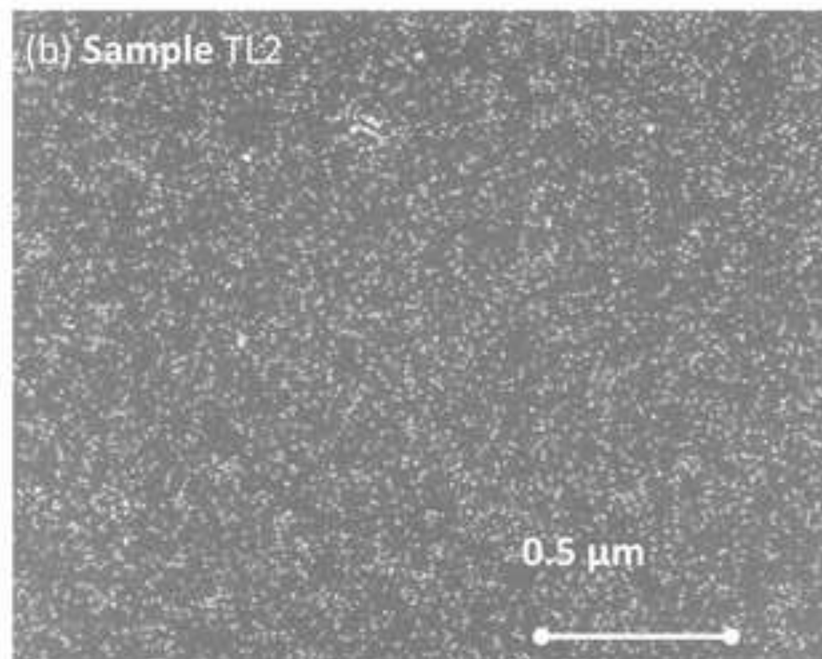

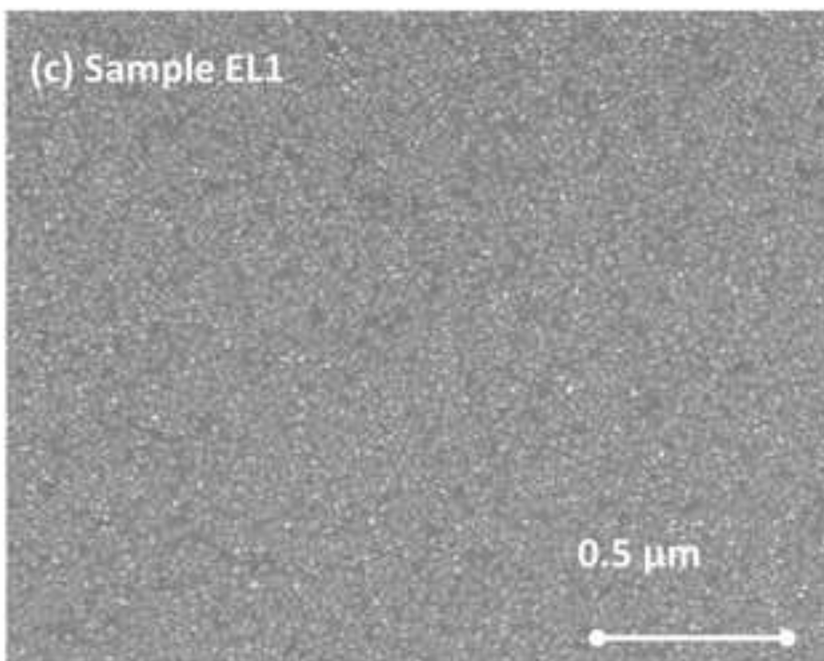

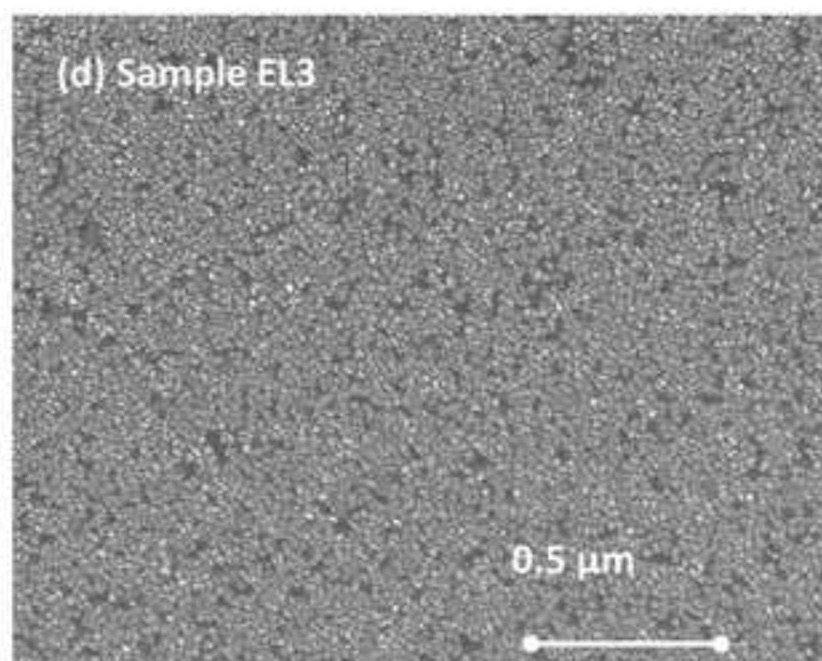

Figure 4

Click here to download Figure Fig4.jpg

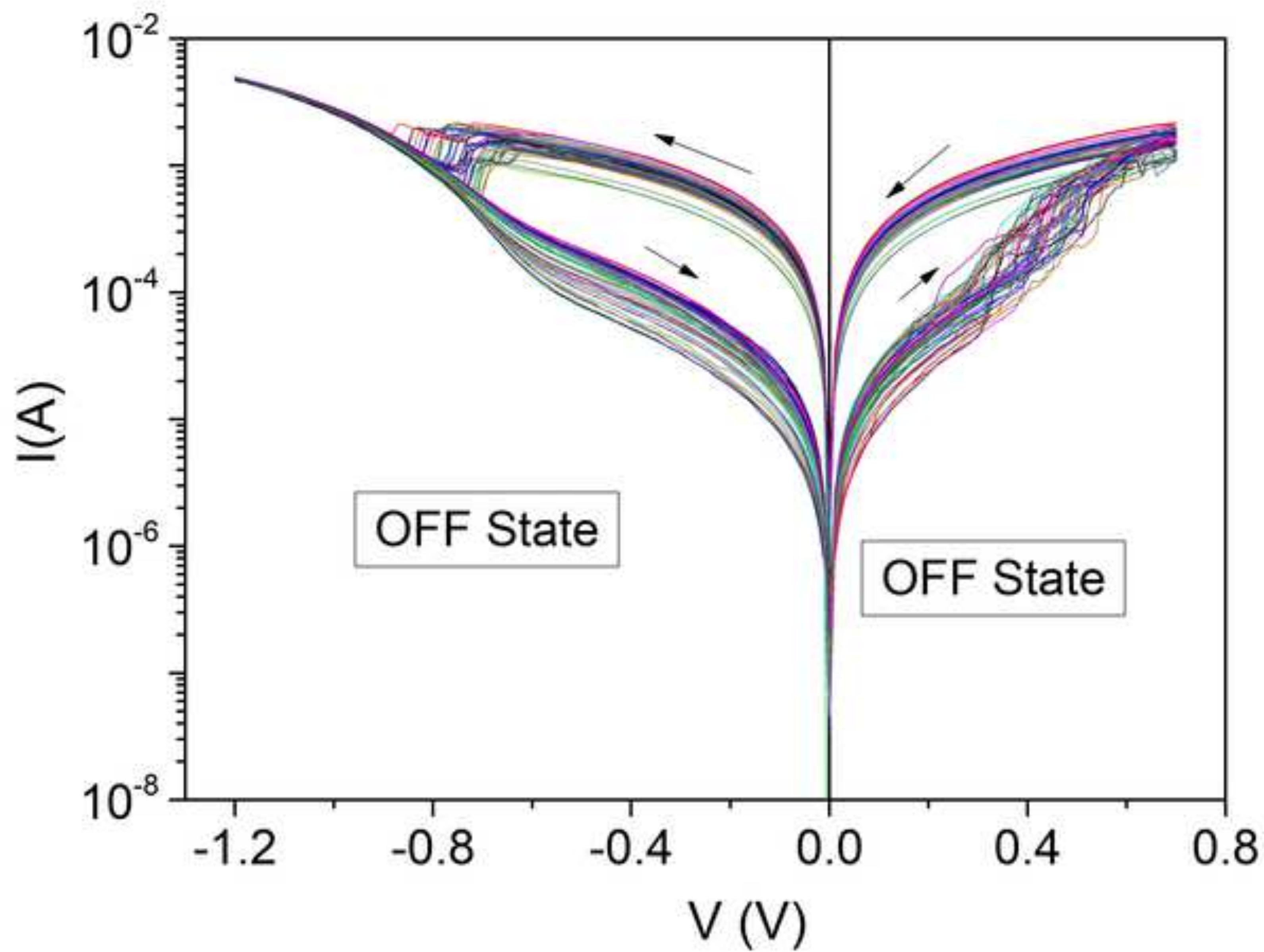

Figure 5 Click here to download Figure Fig5.jpg

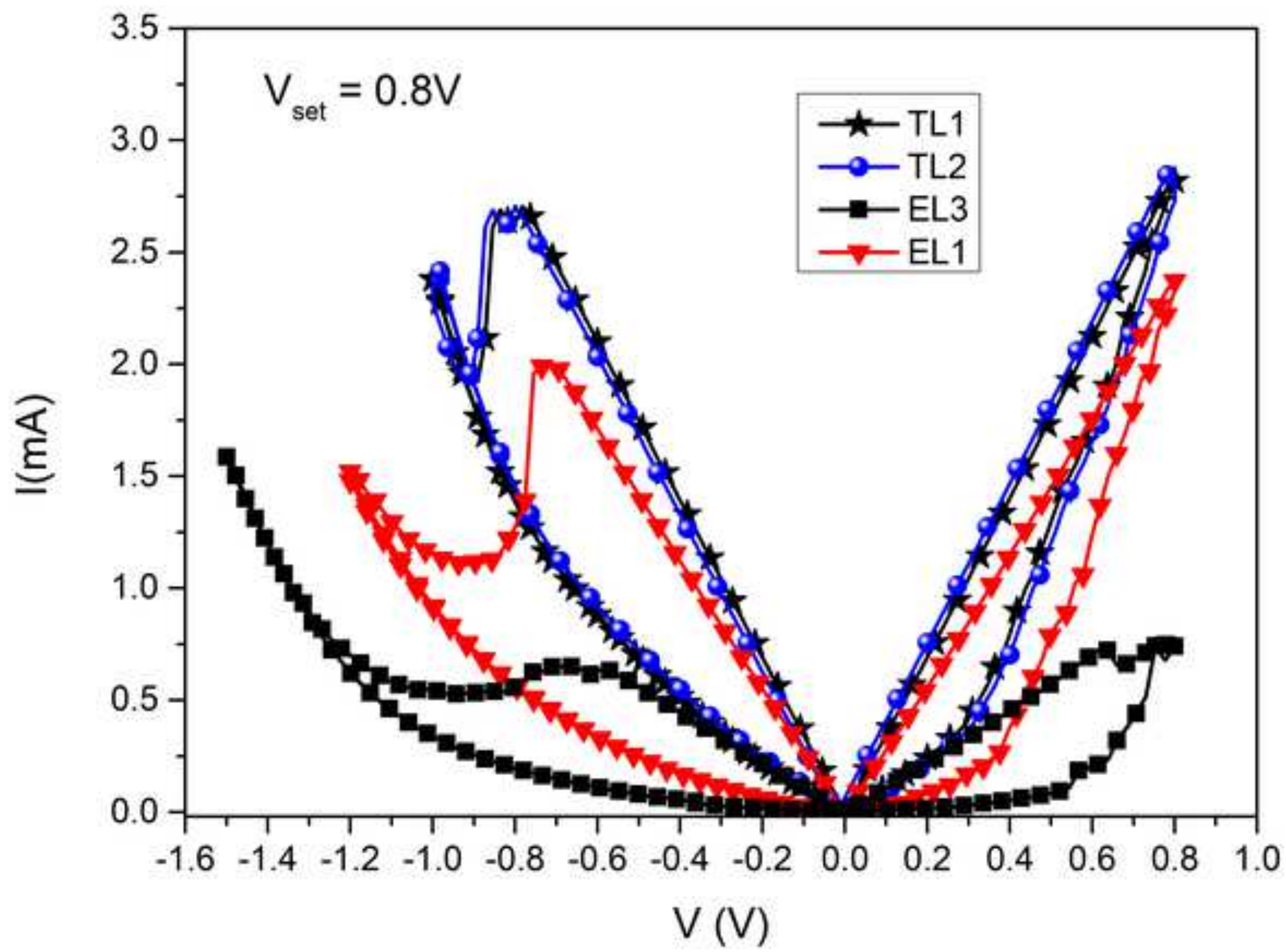

Figure 6

Click here to download Figure Fig6.jpg